

Contribution from the Department of Chemistry,  
Carnegie-Mellon University, Pittsburgh, Pennsylvania 15213

## Photochemical and Thermal Studies of Bis(diethyldithiocarbamato)dioxomolybdenum

MARK W. PETERSON and ROBERT M. RICHMAN\*

Received July 6, 1981

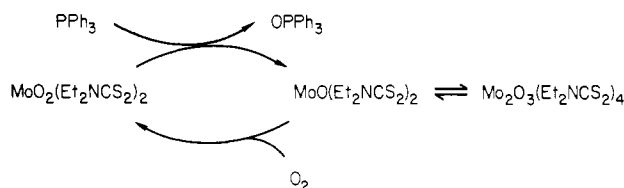
Irradiation at 380 nm into the lowest energy charge-transfer band of  $\text{MoO}_2(\text{Et}_2\text{NCS}_2)_2$  in 1,2-dichloroethane at 23 °C gives  $\text{MoO}_2(\text{Et}_2\text{NCS}_2)$  and  $(\text{Et}_2\text{NCS}_2)_2$  with a quantum yield of 0.0207.  $\text{MoO}_2(\text{Et}_2\text{NCS}_2)$  is identified by its solvent-independent ESR spectrum. A subsequent radical chain reaction occurs in the dark, leading ultimately to a molybdenum oxide and  $(\text{Et}_2\text{NCS}_2)_2$ . Due to these thermal reactions, a plot of loss of  $\text{MoO}_2(\text{Et}_2\text{NCS}_2)_2$  vs. time shows an initial decrease followed by an increase, a behavior that is also dependent on initial concentration. A computer program has been written with use of the fourth-order Runge-Kutta method to simulate this behavior. Several plausible reaction steps are unambiguously eliminated, and a reasonable mechanism that fits all data is proposed.

### Introduction

The literature is rich with studies of molybdenum chemistry. Molybdenum has been shown to exist in oxidation states from -2 to +6 with extensive chemistry known for the states 0-6. Coordination numbers can vary from 4 to 8, and both polynuclear and polymeric forms are known in almost all of the oxidation states.<sup>1</sup>

Recently the utility of Mo(VI) as a redox reagent has become increasingly apparent.<sup>1-12</sup> Molybdenum is known to be a necessary constituent in several complex enzyme systems that catalyze biological redox reactions.<sup>1,13-16</sup> The oxidation states considered most accessible to biological systems are 3-6.

Many studies have been made on simple molybdenum complexes in oxidation states 4-6.<sup>1-20</sup> These studies have demonstrated that the oxidation-state interconversion often involves the formation, loss, or transfer of oxo groups to other molybdenum atoms and/or solvent. Barral et al.<sup>2</sup> first studied the oxygen-transfer reaction of  $\text{MoO}_2((\text{C}_2\text{H}_5)_2\text{NCS}_2)_2$  (**1**) with triphenylphosphine. It was demonstrated that the molybdenum complex played a catalytic role in the presence of oxygen:



Since this work, it has been shown that many other mo-

lybdenum complexes of general form  $\text{MoO}_2\text{L}_2$  (L = bidentate ligand) can be reversibly reduced in the presence of  $\text{O}_2$ .<sup>1-8</sup>

Since molecular excited states have a higher tendency toward both oxidation and reduction than ground states,<sup>21</sup> one might anticipate the generation of still stronger oxidants from irradiation of Mo(VI) complexes. While the photochemistry of lower oxidation states has enjoyed a moderate amount of attention,<sup>22</sup> little work has been done on Mo(VI) complexes with the exception of  $\text{MoOCl}_4$ <sup>23</sup> and  $\text{Mo}(\text{O}_2)_2\text{TTP}$  (TTP = tetraphenylporphine).<sup>24</sup> No photochemistry is reported for the very common  $\text{MoO}_2\text{L}_2$  stoichiometry.

In the present paper we report the photochemistry and subsequent thermal chemistry from irradiation of the sulfur-to-molybdenum charge-transfer band of  $\text{MoO}_2(\text{Et}_2\text{NCS}_2)_2$ . The attainment of a potent and easily regenerated oxidizing agent was not achieved. However, a very interesting decomposition occurs to ultimately form oxides of molybdenum and  $(\text{Et}_2\text{NCS}_2)_2$ . We report the elucidation of a reasonable mechanism to account for the observed chemistry.

### Experimental Section

**Materials and Chemicals.**  $\text{MoO}_2((\text{C}_2\text{H}_5)_2\text{NCS}_2)_2$  was synthesized according to a previously published procedure.<sup>18</sup> After recrystallization from warm benzene/petroleum ether (~50 °C) it was found to contain an ESR-active impurity characteristic of monomeric Mo(V)<sup>25</sup> ( $g_{\text{iso}} = 1.978$ ,  $a_{\text{iso}} = 37$  G). This impurity was eliminated by forming a saturated benzene solution at room temperature, filtering it, and adding ~20% v/v petroleum ether to force ~25% of product out of solution. Anal. Calcd for  $\text{MoO}_2((\text{C}_2\text{H}_5)_2\text{NCS}_2)_2$ : C, 28.30; H, 4.75; N, 6.60; Mo, 22.63. Found: C, 28.35; H, 4.84; N, 6.57; Mo, 22.73.

$\text{Mo}_2\text{O}_4((\text{C}_2\text{H}_5)_2\text{NCS}_2)_2$ <sup>14</sup> and  $((\text{C}_2\text{H}_5)_2\text{NCS}_2)_2$ <sup>26</sup> were synthesized according to previously published procedures. Phenyl-*N-tert*-butylnitron (PBN) was obtained from Aldrich Chemical Co. and used without further purification. Reagent grade 1,2-dichloroethane was distilled and stored over molecular sieves. Reagent grade benzene, toluene, and methylene chloride were used without further purification.

**Quantum Yield Measurements.** All quantum yields were determined in 1,2-dichloroethane. 1,2-Dichloroethane was the chosen solvent for four reasons: (1) **1** is readily soluble in it; (2) **1** is thermally stable over hours in it; (3) it allows UV spectral studies down to 225 nm; (4) while it is prone to radical formation, it should be less so than chloroform or methylene chloride.

In a typical experiment a 2-mL sample of a solution of **1** was deoxygenated with nitrogen and sealed with a rubber septum in a 1-cm

- (1) Steifel, E. I. *Prog. Inorg. Chem.* **1977**, *22*, 1.
- (2) Barral, R.; Bocard, C.; Sere de Roch, I.; Sajus, L. *Kinet. Catal. (Engl. Transl.)* **1973**, *14*, 130.
- (3) Chen, G.; McDonald, J.; Newton, W. *Inorg. Chem.* **1976**, *15*, 2612.
- (4) Durant, R.; Garner, C.; Hyde, M.; Mabbs, F. *J. Chem. Soc., Dalton Trans.* **1977**, 955.
- (5) Sawyer, D.; Howie, J.; Daub, W. *J. Less-Common Met.* **1977**, *54*, 425.
- (6) Durant, R.; Garner, C.; Hyde, M.; Mabbs, F.; Parsons, J.; Richens, D. *J. Less-Common Met.* **1977**, *54*, 459.
- (7) Speier, G. *Inorg. Chim. Acta* **1979**, *32*, 139.
- (8) Matsuda, T.; Tanaka, K.; Tanaka, T. *Inorg. Chem.* **1979**, *18*, 454.
- (9) de Hayes, L. J.; Faulkner, H. C.; Doub, W. H., Jr.; Sawyer, D. T. *Inorg. Chem.* **1975**, *14*, 2110.
- (10) Taylor, R. D.; Street, J. P.; Minelli, M.; Spence, J. T. *Inorg. Chem.* **1978**, *17*, 3207.
- (11) Cliff, C. A.; Fallon, G. D.; Gatehouse, B. M.; Murray, K. S.; Newman, P. J. *Inorg. Chem.* **1980**, *19*, 773.
- (12) Topich, J. *Inorg. Chem.* **1981**, *20*, 3704.
- (13) Spece, J. *Coord. Chem. Rev.* **1969**, *4*, 475.
- (14) Newton, W.; Corbin, J.; Bravard, D.; Searles, J.; McDonald, J. *Inorg. Chem.* **1974**, *13*, 1100.
- (15) Watt, G.; McDonald, J.; Newton, W. *J. Less-Common Met.* **1977**, *54*, 415.
- (16) Sykes, A. G. *J. Less-Common Met.* **1977**, *54*, 401.
- (17) Mitchell, P. Q. *Rev., Chem. Soc.* **1966**, *20*, 103.
- (18) Moore, F.; Larson, M. *Inorg. Chem.* **1967**, *6*, 998.
- (19) Moore, F.; Rice, R. *Inorg. Chem.* **1968**, *7*, 2510.
- (20) Jowitt, R.; Mitchell, P. *J. Chem. Soc. A* **1970**, 1702.

- (21) Creutz, C.; Sutin, N. *J. Am. Chem. Soc.* **1976**, *98*, 6384.
- (22) See, for example: Balzani, V.; Carassiti, V. "Photochemistry of Coordination Compounds"; Academic Press: London, 1970. Geoffroy, G.; Wrighton, M. S. "Organometallic Photochemistry"; Academic Press: London, 1979. Adamson, A.; Fleischauer, P. "Concepts of Inorganic Photochemistry"; Wiley: New York, 1975.
- (23) Larson, M.; Moore, F. *Inorg. Chem.* **1966**, *5*, 801.
- (24) Ledon, H.; Bonnet, M.; Lallemand, J.-Y. *J. Chem. Soc., Chem. Commun.* **1979**, 702.
- (25) See ref 1, pp 70, 71.
- (26) Deronzier, A.; Meyer, T. J. *Inorg. Chem.* **1980**, *19*, 2912.

quartz cell. The sample was then irradiated at 380 nm with a Hanovia 1000-W mercury-xenon lamp by using a Bausch & Lomb high-intensity grating monochromator. Spectral changes were monitored from 800 to 230 nm on a Perkin-Elmer Model 330 UV-visible spectrophotometer. Since typical optical densities at 380 nm were much less than 2, it was necessary to integrate the quantum yield equation, yielding<sup>27</sup>

$$\phi_0 = \frac{1}{I_0 t} \left( [1]_0 - [1] + \frac{1}{2.303 \epsilon_1 b} \ln \left( \frac{1 - e^{-2.303 \epsilon_1 b [1]_0}}{1 - e^{-2.303 \epsilon_1 b [1]}} \right) \right)$$

where  $I_0$  is the lamp intensity as determined by standard ferrioxalate actinometry,  $t$  is the irradiation time,  $[1]_0$  is the initial concentration of **1**,  $[1]$  is the concentration of **1** after irradiation,  $\epsilon_1$  is the extinction coefficient of **1** at 380 nm, and  $b$  is the cell path length.

All measurements were done at  $23.0 \pm 0.5$  °C. Thermal blanks were also run at  $23.0 \pm 0.5$  °C to insure the stability of **1** over the period of the experiment.

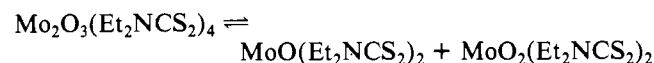
**Instruments.** All UV-visible spectra were recorded on a Perkin-Elmer Model 330 spectrophotometer that has been interfaced to a Digital Equipment Corp. MINC-11 computer. ESR spectra were recorded on a Varian E-4 spectrometer. Illumination into the ESR cavity was done by using a 300-W tungsten projector lamp with a Corning 3-75 cutoff filter. IR spectra were recorded on a Perkin-Elmer Model 580 spectrophotometer that has been interfaced to a Perkin-Elmer CDS-2 data station.

**Kinetic Fits.** For the simulation of the concentration variation of **1** for various mechanisms a computer program has been written based on the fourth-order Runge-Kutta method<sup>28</sup> for obtaining approximate solutions to a system of first-order differential equations given initial values. The program is written to simulate both photolytic and thermal reactions for an experimental time. Then the photolytic processes are "turned off" and the thermal processes allowed to continue for 2 min (approximately the time necessary to remove a sample from the lamp and record its spectrum). The quality of a given fit was determined by the standard deviation between experimental and calculated values of  $[1]$ . Rate constants were calculated from experimental results when possible; otherwise, estimates and educated guesses were used as initial values. The rate constants were then varied to minimize the standard deviation.

## Results and Discussion

The lowest energy visible transition for **1** is at 380 nm. Several authors have assigned this transition as a sulfur-to-molybdenum charge transfer,<sup>18-20</sup> however, more recently, Newton et al.<sup>14</sup> have assigned it as an oxygen-to-molybdenum CT.

The basis for the oxygen-to-molybdenum CT assignment was the experimental observation that despite the equilibrium for  $\text{Mo}_2\text{O}_3(\text{Et}_2\text{NCS}_2)_4$  ( $K_{\text{eq}} = 2 \times 10^{-3} \text{ M}^8$ )



the apparent extinction coefficient at 380 nm remains constant over a relatively large initial concentration range of  $\text{Mo}_2\text{O}_3(\text{Et}_2\text{NCS}_2)_4$ . Experimentally this is explained by the fact that  $\epsilon(\text{MoO}(\text{Et}_2\text{NCS}_2)_2) \cong \frac{1}{3}\epsilon(\text{Mo}_2\text{O}_3(\text{Et}_2\text{NCS}_2)_4)$  and  $\epsilon(\text{MoO}_2(\text{Et}_2\text{NCS}_2)_2) \cong \frac{2}{3}\epsilon(\text{Mo}_2\text{O}_3(\text{Et}_2\text{NCS}_2)_4)$ . Hence, it appears that the extinction coefficient at 380 nm is a linear function of the number of oxygen atoms. This then was the rationale for the assignment.<sup>14</sup>

We take exception to the oxygen-to-molybdenum CT assignment for four reasons and wish to reassign it as a sulfur-to-molybdenum CT. First, sulfur is more easily oxidized than oxygen. Second, in a theoretical calculation on a model oxo-bridged Mo(V) dithiocarbamate dimer, a transition is calculated at  $\sim 390$  nm, which may be assigned as a sulfur-to-molybdenum CT.<sup>29</sup> Third, a survey of Table V in ref 1

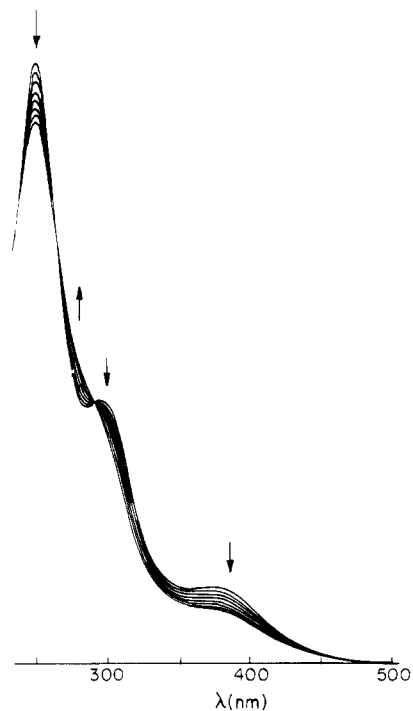


**Figure 1.** Spectral changes of  $\text{MoO}_2(\text{Et}_2\text{NCS}_2)_2$  during photolysis at 380 nm in 1,2-dichloroethane. Spectra are taken at 5-min intervals.

**Table I.** Isotropic  $g$  and Hyperfine ( $^{95,97}\text{Mo}$ ) Constants for Transient Mo(V) in Various Solvents

solvent	$g_{\text{iso}}$	$a_{\text{iso}}, \text{G}$	solvent	$g_{\text{iso}}$	$a_{\text{iso}}, \text{G}$
1,2-dichloroethane	$1.952 \pm 0.002$	$42 \pm 2$	benzene	1.952	42
			toluene	1.952	42
methylene chloride	1.951	42			

and Table I in ref 12 shows that the lowest energy absorptions for many Mo(VI) *cis*-dioxo complexes are at wavelengths substantially smaller than 380 nm. And, finally, the results reported here show that the primary photostep is what would be expected for ligand-to-metal charge-transfer photochemistry involving the dithiocarbamate ligand.

Irradiation of an initially yellow solution of **1** at 380 nm causes a slow bleaching. At concentrations of  $\sim 10^{-3} \text{ M}$  this bleaching is accompanied by formation of a gray precipitate that has been isolated. Energy-dispersive analysis by X-rays of the precipitate isolated from both 1,2-dichloroethane and benzene shows only the presence of molybdenum with no noticeable sulfur (from the ligand) or chlorine (from the solvent in the first case). Both samples have weak IR absorptions consistent with  $\text{MoO}_2$ ;<sup>30</sup> however, their X-ray powder diffraction patterns, while virtually identical with one another, have  $d$  spacings that cannot be assigned to any known molybdenum oxide.<sup>31</sup> The bleached solution is found to contain  $((\text{C}_2\text{H}_5)_2\text{NCS}_2)_2$  (UV:  $\lambda_{\text{max}} = 290 \text{ nm}$ ,  $\epsilon = 1.23 \times 10^4 \text{ cm}^{-1} \text{ M}^{-1}$ ). While the ultimate fate of **1** is known, it was the mechanism of this process that interested us.

The spectral changes during photolysis of **1** at 380 nm in 1,2-dichloroethane are shown in Figure 1. It can be seen that the peaks due to **1** ( $\lambda_{\text{max}} = 258, 300, 380 \text{ nm}$ ;  $\epsilon = 28, 100, 12,600, 3700 \text{ cm}^{-1} \text{ M}^{-1}$ ) diminish with irradiation time while there is a growth at  $\sim 290 \text{ nm}$ . Isosbestic points are maintained at  $\lambda = 295, 268, \text{ and } 242 \text{ nm}$ . If the molar extinction

(27) Kling, Von O.; Nikolaïski, E.; Schlafer, H. *Ber. Bunsenges. Phys. Chem.* **1963**, *67*, 883.

(28) Rolston, A.; Wilf, H. "Mathematical Methods and Digital Computers"; Wiley: New York, 1960; pp 110-120.

(29) Blues, B.; Brown, D. H.; Perkins, P. G.; Stewart, J. J. P. *Inorg. Chim. Acta* **1974**, *8*, 67.

(30) Parodi, M. C. R. *Hebd. Seances Acad. Sci.* **1937**, *205*, 906.

(31) "1979 Powder Diffraction File of Inorganic Materials"; International Center for Diffraction Data: Swarthmore, PA, 1979.

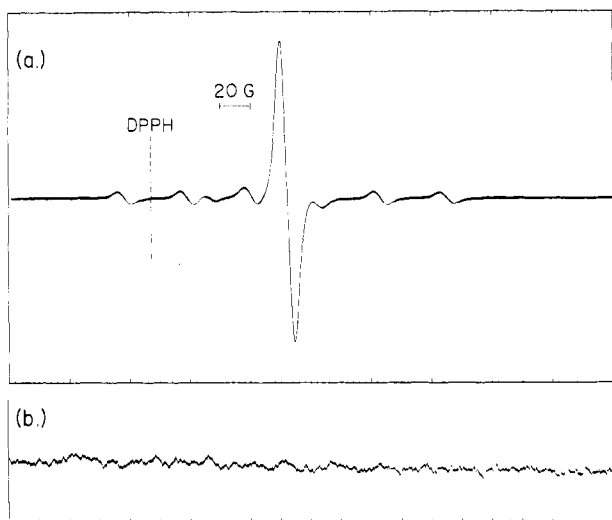


**Figure 2.** Ambient ESR spectrum of  $\text{MoO}_2(\text{Et}_2\text{NCS}_2)_2$  in 1,2-dichloroethane (a) with lamp on and (b) after lamp has been off for 1 min. The scan is from 3300 to 3700 G at 9.52 GHz. The receiver gain is (a) 320 and (b) 10000.

coefficients of **1** and  $(\text{Et}_2\text{NCS}_2)_2$  are plotted vs. wavelength, the curves are found to intersect at  $\lambda = 295, 268,$  and  $242$  nm, consistent with the stoichiometry  $\mathbf{1} \rightarrow (\text{Et}_2\text{NCS}_2)_2 + \text{MoO}_2$ .

In order to verify that all postphotolytic thermal chemistry has stopped by the time the UV spectrum is recorded, we ran a sample in which the absorbances at 380, 300, and 258 nm were monitored over a period of 30 min between irradiations. No changes within experimental error were observed during these 30-min periods.

A solution of **1** irradiated in an ESR spectrometer produces a signal typical of monomeric  $\text{Mo(V)}^{25}$  (Figure 2a). Identical signals can be produced in a variety of solvents (Table I), implying that the  $\text{Mo(V)}$  does not incorporate solvent. When irradiation is stopped, the  $\text{Mo(V)}$  signal decays rapidly and ultimately disappears (Figure 2b).

Addition of an excess of PBN to a degassed solution of **1** in benzene or 1,2-dichloroethane followed by irradiation in an ESR cavity over a period of 2 h leads to a signal typical of a nitron adduct. The coupling parameters are  $a_{\beta}^{\text{H}} = 2.4$  G and  $a_{\beta}^{\text{N}} = 14.8$  G in benzene and 2.4 and 14.7 G in 1,2-dichloroethane. We assign this to the  $\text{Et}_2\text{NCS}_2$  adduct of PBN.

The UV and ESR results are not consistent with a primary photochemical step involving activation and abstraction of an oxygen atom from **1**. Oxygen abstraction would lead to  $\text{MoO}(\text{Et}_2\text{NCS}_2)_2$  and hence  $\text{Mo}_2\text{O}_3(\text{Et}_2\text{NCS}_2)_4$ , which has a characteristic absorption at 510 nm.<sup>1</sup> This is not observed spectroscopically. Even small amounts of  $\text{Mo}_2\text{O}_3(\text{Et}_2\text{NCS}_2)_4$  would destroy any isosbestic points. Dissociation of  $\text{Et}_2\text{NCS}_2$  rather than oxygen is an apparent contradiction with Topich's conjecture<sup>12</sup> that these compounds lose oxygen upon electrochemical one-electron reduction. However, the oxidized  $\text{Et}_2\text{NCS}_2$  present in the photochemical experiment initiates a series of reactions that may be fast with respect to oxygen atom loss (vide infra). Indeed, some oxygen loss may be responsible for the nonstoichiometric nature of the final molybdenum oxide.

The quantum yield for disappearance of **1** was measured and found not to be constant with time. Rather it showed an initial steep descent followed by a slow upward trend. Figure 3 shows this quantum yield variation for three different initial concentrations of **1**. It can be seen that the nature of this variation is strongly dependent on the starting concentration of **1**.

These results are puzzling in two respects. First, for the maintenance of isosbestic points consistent with **1** and

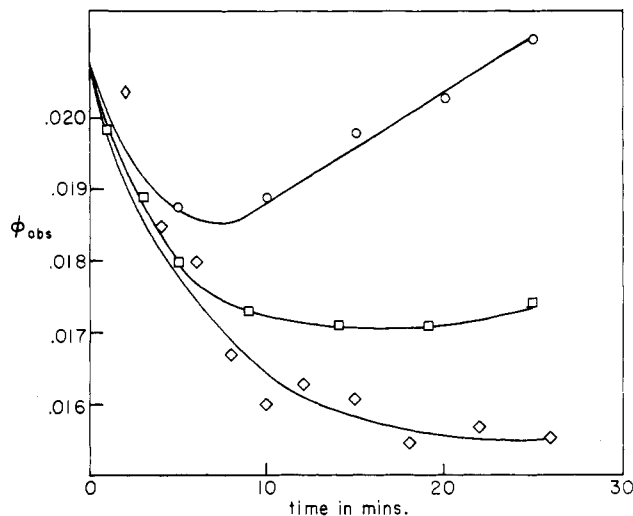
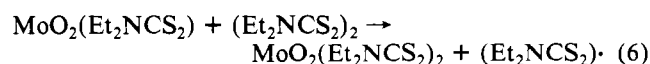
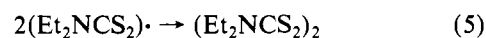
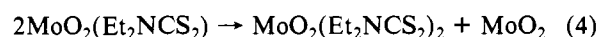
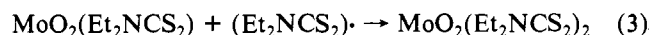
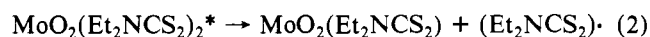
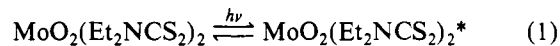


**Figure 3.** Quantum yield for loss of  $\text{MoO}_2(\text{Et}_2\text{NCS}_2)_2$  vs. time for three different initial concentrations: (O)  $9.5 \times 10^{-5}$  M; ( $\square$ )  $6.5 \times 10^{-5}$  M; ( $\diamond$ )  $5.7 \times 10^{-5}$  M.  $I_0 = 3.2 \times 10^{-9}$  einstein.

$(\text{Et}_2\text{NCS}_2)_2$  as the sole absorbing species, there must be some process either photochemical or thermal by which **1** loses both its ligands with a  $\text{Mo(V)}$  intermediate. Second, the quantum yield variation shows a radical change in its nature that depends on the initial concentration of **1**.

The initial drop in the disappearance of quantum yield with time is not hard to explain. One obvious explanation would be excited-state quenching of **1** by the photoproducts. However, **1** shows no emission at room temperature or 77 K below 800 nm. This explanation would also require an unreasonably long lifetime for the excited state. A second more reasonable explanation is reaction of the initial photoproducts to produce **1**. This seems reasonable for three reasons. First, both  $\text{Mo(V)}$  and  $\text{Et}_2\text{NCS}_2$  represent transient products that are thermodynamically unstable. Second, this type of behavior has been observed in an analogous complex.<sup>32</sup> Finally, this is supported by the intensity dependence. If two identical samples are irradiated, one at  $I_0$  and the other at  $2I_0$ , an apparent decrease in the observed quantum yields at early time is found for the higher lamp intensity relative to that for the lower. This observation is consistent with an increase in the rate of some reaction that produces **1**.

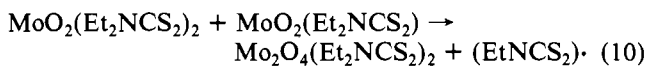
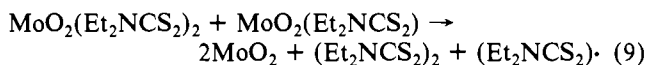
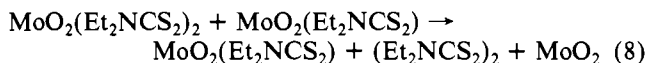
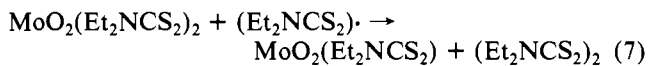
This back-reaction can take three possible forms—steps 3, 4, and 6 in the following scheme. Step 6 has been eliminated since photolysis of **1** with added  $(\text{Et}_2\text{NCS}_2)_2$  shows no change in the initial drop of the quantum yield.



After the initial drop, the quantum yield begins to flatten out and even increase with time at high concentrations of **1**. This rise in the quantum yield is indicative of some thermal process that begins to consume **1**. Separate experiments with added  $(\text{Et}_2\text{NCS}_2)_2$  and  $\text{MoO}_2$  show no acceleration of this

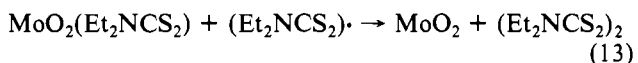
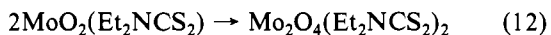
(32) Unpublished result for  $\text{MoO}_2\text{L}_2$ , where L = dibenzoylmethane.

thermal reaction. Hence, there must be reaction with either  $\text{MoO}_2(\text{Et}_2\text{NCS}_2)$  or  $(\text{Et}_2\text{NCS}_2)$ . The reactions we have considered are given by eq 7–10.

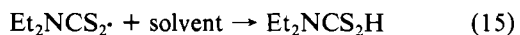
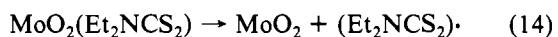


To test step 10, we prepared a sample of the known  $\text{Mo}_2\text{O}_4(\text{Et}_2\text{NCS}_2)_2$  independently. Photolysis of a solution of  $\text{Mo}_2\text{O}_4(\text{Et}_2\text{NCS}_2)_2$  shows that it is photoinert at 380 nm ( $\phi_0 < 10^{-3}$ ). Furthermore, there is no spectroscopic evidence for formation of  $\text{Mo}_2\text{O}_4(\text{Et}_2\text{NCS}_2)_2$ . Hence, step 10 can be eliminated. It should be noted that in an electrochemical study of **1** in  $\text{Me}_2\text{SO}$  the ultimate products upon a one-electron reduction are  $(\text{Et}_2\text{NCS}_2)_2$  and  $\text{Mo}_2\text{O}_4(\text{Et}_2\text{NCS}_2)_2$ .<sup>9</sup> This result is not disturbing since in  $\text{Me}_2\text{SO}$  **1** undergoes a dimerization to  $\text{Mo}_2\text{O}_4(\text{Et}_2\text{NCS}_2)_4$ . This is then reduced to  $\text{Mo}_2\text{O}_4(\text{Et}_2\text{NCS}_2)_2$ , so the  $\text{MoO}_2(\text{Et}_2\text{NCS}_2)$  reactive intermediate is never present. This then implies that the rate of  $(\text{Et}_2\text{NCS}_2) \cdot$  reaction with  $\text{Mo}_2\text{O}_4(\text{Et}_2\text{NCS}_2)_2$  is probably substantially less than the rate of dimerization of  $\text{Et}_2\text{NCS}_2$ , perhaps because formation of  $(\text{Et}_2\text{NCS}_2)_2$  is intramolecular.<sup>9</sup>

Of the possible reactions proposed so far, steps 4, 8, and 9 yield the ultimate product  $\text{MoO}_2$ . However, other possibilities must be considered. One might speculate that  $\text{MoO}_2(\text{Et}_2\text{NCS}_2)$  undergoes photolysis to  $\text{MoO}_2$  and  $(\text{Et}_2\text{NCS}_2) \cdot$ . However, this is inconsistent with the ESR results.  $\text{Mo(V)}$  disappears after the irradiation is stopped. Flash photolysis experiments<sup>33</sup> indicate a transient–transient reaction with  $k/\epsilon = 1.5 \times 10^6 \text{ cm s}^{-1}$ . The observed transient can be assumed to be  $\text{Mo(V)}$  since  $(\text{Et}_2\text{NCS}_2) \cdot$  has been shown to have no strong absorption bands in the visible region.<sup>26</sup> Steps 3 and 4 are two possible transient–transient reactions. Other possible reactions are given by eq 11–13. Step 12 can be eliminated, since the stable  $\text{Mo}_2\text{O}_4(\text{Et}_2\text{NCS}_2)_2$  is not observed.



Finally, there are two more potential reactions that must be considered, which are given by eq 14 and 15. Step 15 can be eliminated since there is no spectroscopic evidence for either  $\text{Et}_2\text{NCS}_2\text{H}$  or its decomposition products,  $\text{CS}_2$  and  $\text{Et}_2\text{NH}$ .



For the further resolution of which of these reactions are actually taking place in this system the continuous photolysis data were simulated with a kinetic program based on the fourth-order Runge–Kutta algorithm (RK4) for solution to a set of coupled linear differential equations. The goal is to fit the variation in the concentration of **1** for all experiments by using the same rate constants with a minimum number of reactions.

Steps 8 and 9 have been eliminated on the basis of these results. Taking either step 8 or 9 and an appropriate reaction

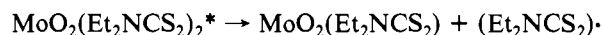
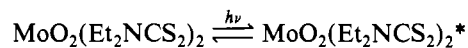
for regeneration of **1** (step 3 or 4), it is possible to fit the concentration variation of **1** at late time; however, it is then impossible to fit the data at early time. This is not an unreasonable result for step 8, since this reaction is competitive with the regeneration reaction necessary for fitting early time results. It is not as clear why step 9 should fail. If the early time variation is first fit and then step 9 added to fit later times, the initial fit is lost and cannot be restored. The fundamental problem is that, for the proper concentrations of  $\text{MoO}_2(\text{Et}_2\text{NCS}_2)$  to allow the regeneration reaction to proceed at a proper rate, either step 9 will dominate both early and late times or it will be insufficient to produce proper late time results.

Step 4 may be eliminated on the basis of both ESR results and the computer fits. If a sample is irradiated in an ESR tube in the presence of a good hydrogen atom donor (cumene), the signal due to  $\text{Mo(V)}$  does not completely disappear. This result is more consistent with step 3 than with step 4. Furthermore, it is not possible to reproduce the observed minima in Figure 3 if step 4 is used as the primary quenching step.

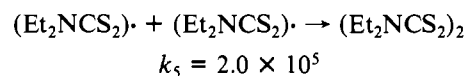
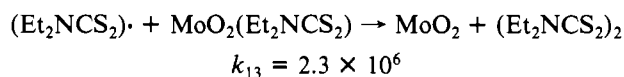
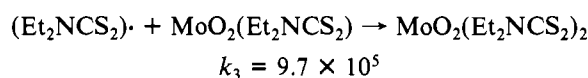
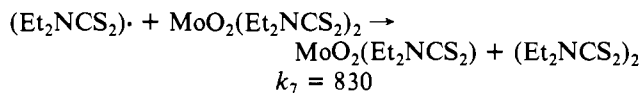
The ultimate fate of  $\text{MoO}_2(\text{Et}_2\text{NCS}_2)_2$  must be  $\text{MoO}_2$ . There are three remaining reactions that will allow this (steps 11, 13, and 14). Any of these three steps gives a good fit for any single experiment. However, when steps 11 and 14 were used, it was necessary to vary  $k_{11}$  or  $k_{14}$  to obtain good fits. These rate constants must increase with increasing starting concentration of **1**. Only step 13 allows for simultaneous fits of five separate experiments. This is also consistent with the thermal decay of  $\text{Mo(V)}$  observed by ESR.

Figure 4 shows the experimental concentration of **1** vs. the concentrations obtained from the RK4 fits for four experiments using the reactions and rate constants given in Mechanism I. These rate constants are not necessarily unique. If  $k_5$  (a literature value)<sup>34</sup> is allowed to decrease,  $k_3$ ,  $k_7$ , and  $k_{13}$  may be increased to acquire good fits.

#### Mechanism I



$$I_m, \phi_0 = 0.0207$$



An attempt was made to simplify the system by reducing the temperature to 0 and  $-78^\circ\text{C}$  to eliminate postphotolytic thermal reactions. Surprisingly, the photochemistry at low temperature is more complex than that at room temperature.

Irradiation of **1** in 1,2-dichloroethane at  $0^\circ\text{C}$  leads to formation of  $\text{Mo}_2\text{O}_3(\text{Et}_2\text{NCS}_2)_4$  (IR 739, 436  $\text{cm}^{-1}$ ; vis 514 nm). However, this formation is not quantitative; that is, not all of Mo is present as  $\text{MoO}_2(\text{Et}_2\text{NCS}_2)_2$ ,  $\text{MoO}(\text{Et}_2\text{NCS}_2)_2$ , and  $\text{Mo}_2\text{O}_3(\text{Et}_2\text{NCS}_2)_4$ . No isobestic points are observed, and at long irradiation time the  $\text{Mo}_2\text{O}_3(\text{Et}_2\text{NCS}_2)_4$  begins to disappear. A photolyzed solution exhibits three  $\text{Mo(V)}$  ESR

(33) Peterson, M. W.; Richman, R. M.; Ferraudi, G., submitted for publication in *Inorg. Chem.*

(34) Cauguis, G.; Lachenal, D. *J. Electroanal. Chem. Interfacial Electrochem.* 1973, 43, 405.

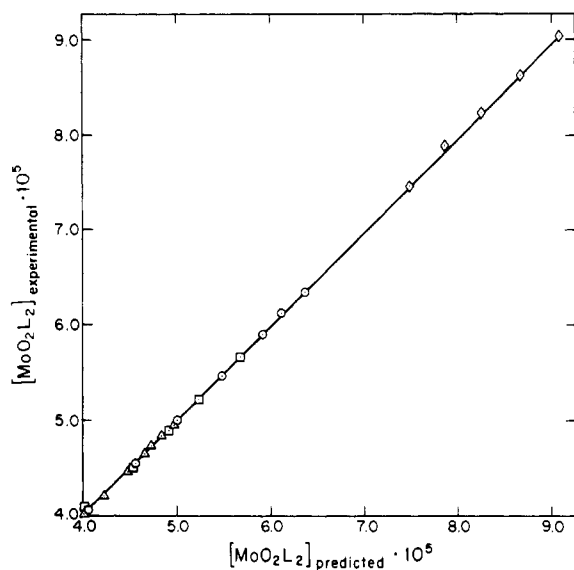


**Figure 4.** Plot of experimental values of  $\text{MoO}_2(\text{Et}_2\text{NCS}_2)_2$  vs. predicted values from the computer fits for four different initial concentrations: ( $\diamond$ )  $9.5 \times 10^{-5}$  M; ( $\square$ )  $5.7 \times 10^{-5}$  M; ( $\triangle$ )  $4.5 \times 10^{-5}$  M,  $I_0 = 3.2 \times 10^{-9}$  einstein; ( $\circ$ )  $6.5 \times 10^{-5}$  M,  $I_0 = 5.4 \times 10^{-9}$  einstein.

signals ( $^1g_{\text{iso}} = 1.978$ ,  $^1a_{\text{iso}} = 37$  G;  $^2g_{\text{iso}} = 1.966$ ,  $^2a_{\text{iso}} = 39$  G;  $^3g_{\text{iso}} = 1.953$ ,  $^3a_{\text{iso}} = 41$  G). These signals are stable over

hours in degassed solution. Ultraviolet and infrared spectroscopy indicates that  $\text{MoO}_2(\text{Et}_2\text{NCS}_2)_2$  reacts with  $\text{Et}_2\text{NCS}_2\text{H}$  to form  $\text{Mo}_2\text{O}_3(\text{Et}_2\text{NCS}_2)_4$  in moderate yields. The ESR of the reaction mixture shows two Mo(V) signals at  $g_{\text{iso}} = 1.965$ ,  $a_{\text{iso}} = 39$  G and  $g_{\text{iso}} = 1.977$ ,  $a_{\text{iso}} = 37$  G.

On the basis of the above results we postulate that at low temperatures hydrogen atom abstraction from either solvent or other ligands becomes competitive with other possible ligand radical reactions.

### Conclusions

We have demonstrated for the first time the ability of a Mo(VI) complex of the very common form  $\text{MoO}_2\text{L}_2$  to do redox photochemistry. The primary photostep can be assumed to be thermodynamically uphill since step 3 must be included in the ultimate mechanism. The driving force toward decomposition appears to be the stability of  $(\text{Et}_2\text{NCS}_2)_2$ . The radical chain mechanism provides an efficient kinetic pathway to the final products. The RK4 method is a useful way for the kineticist to eliminate possible reaction steps.

**Acknowledgment.** We thank Mr. Reuel Van Atta for experimental assistance, Mr. Howard Wagenblast of the Mellon Institute for EDAX and X-ray diffraction results, and Professor Patrick M. McCurry for helpful discussions. Financial support of the Office of Basic Energy Sciences, Department of Energy, is gratefully acknowledged.

Registry No. 1, 18078-69-8.

Contribution from the Department of Chemistry, Northeastern University, Boston, Massachusetts 02115

## Thiocyanate-Bridged Transition-Metal Polymers. 3. Structure and Low-Temperature Magnetic Properties of $\text{Ni}(\text{bpy})(\text{NCS})_2$ : An Infinite-Chain Ferromagnetic Insulator

BRUCE W. DOCKUM and WILLIAM MICHAEL REIFF\*

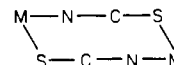
Received October 12, 1981

The new compound  $\text{Ni}(\text{bpy})(\text{NCS})_2$  (bpy = 2,2'-bipyridine) has been prepared by the stepwise thermolytic decomposition of  $\text{Ni}(\text{bpy})_3(\text{NCS})_2 \cdot 3\text{H}_2\text{O}$  with  $\text{Ni}(\text{bpy})_2(\text{NCS})_2$  as an intermediate product. Studies by optical and infrared spectroscopy indicate that  $\text{Ni}(\text{bpy})(\text{NCS})_2$  is a polymer with six-coordinate metal centers and bridging thiocyanate anions. The structure is proposed to have either zigzag or helical chains each containing stepwise, metal-thiocyanate bridging groups. Variable-temperature magnetic susceptibility measurements in a field of 1.69 kG show the presence of relatively strong ferromagnetic interactions, i.e., a rapid increase in the moment until a maximum value of  $8.4 \mu_B$  is obtained at  $\sim 3.5$  K. The susceptibility exhibits a very rapid rise until  $\sim 2$  K at which it levels off. From the susceptibility behavior, it is shown that  $\text{Ni}(\text{bpy})(\text{NCS})_2$  orders as a ferromagnet with  $T_c = 3.5$  K.

### Introduction

In previous articles,<sup>1-4</sup> we have reported the structural and magnetic properties for some first transition-metal series diimine compounds having the empirical formula  $\text{M}(\text{bpy})(\text{NCS})_2$  (M is divalent Fe, Co, Mn, and Cu; bpy = 2,2'-bipyridine). X-ray powder patterns of each system have revealed

structural isomorphism between the manganese, iron, and cobalt compounds and a different pattern for  $\text{Cu}(\text{bpy})(\text{NCS})_2$ .<sup>5</sup> The available spectral data including optical, infrared, EPR, and Mössbauer spectroscopy indicate that  $\text{Fe}(\text{bpy})(\text{NCS})_2$ <sup>2,4</sup> and its Mn and Co analogues<sup>3</sup> are polymers in which all the thiocyanate groups are bridging forming zigzag chains of stepwise, near-orthogonal



bridging groups. The structure of these compounds is believed

- (1) W. M. Reiff, H. Wong, B. Dockum, T. Brennan, and C. Cheng, *Inorg. Chim. Acta.*, **30**, 69 (1978).
- (2) W. M. Reiff, B. Dockum, C. Torardi, H. Wong, and S. Foner, paper presented at the 168th National Meeting of the American Chemical Society, Atlantic City, NJ, Sept 1974, No. 82.
- (3) B. W. Dockum and W. M. Reiff, paper presented at the Second Joint Conference of the CIC and ACS, Montreal, Canada, May 1977, No. 9.
- (4) B. W. Dockum and W. M. Reiff, *Inorg. Chem.*, **21**, 391, 1406 (1982).

- (5) B. W. Dockum, Ph.D. Dissertation, Department of Chemistry, Northeastern University, Boston, MA, 1977.